RESEARCH ARTICLE | MARCH 31 2014

Evaluation of the threshold trimming method for micro inertial fluidic switch based on electrowetting technology

Tingting Liu; Wei Su; Tao Yang; Bin Han

AIP Advances 4, 037126 (2014)
https://doi.org/10.1063/1.4870243

AIP ADVANCES **4**, 037126 (2014)

Evaluation of the threshold trimming method for micro inertial fluidic switch based on electrowetting technology

Tingting Liu,[1,2,3,a] Wei Su,[2] Tao Yang,[3] and Bin Han[3]
[1]*School of Physical Sciences, University of Science and Technology of China, Hefei, 230026, Anhui province, China*
[2]*Institute of Electronic Engineering, China Academy of Engineering Physics, Mianyang, 621000, Sichuan province, China*
[3]*Robot Technology Used for Special Environment Key Laboratory of Sichuan Province, Southwest University of Science and Technology, Mianyang, 621000, Sichuan province, China*

(Received 7 January 2014; accepted 19 March 2014; published online 31 March 2014)

The switch based on electrowetting technology has the advantages of no moving part, low contact resistance, long life and adjustable acceleration threshold. The acceleration threshold of switch can be fine-tuned by adjusting the applied voltage. This paper is focused on the electrowetting properties of switch and the influence of microchannel structural parameters, applied voltage and droplet volume on acceleration threshold. In the presence of process errors of micro inertial fluidic switch and measuring errors of droplet volume, there is a deviation between test acceleration threshold and target acceleration threshold. Considering the process errors and measuring errors, worst-case analysis is used to analyze the influence of parameter tolerance on the acceleration threshold. Under worst-case condition the total acceleration threshold tolerance caused by various errors is 9.95%. The target acceleration threshold can be achieved by fine-tuning the applied voltage. The acceleration threshold trimming method of micro inertial fluidic switch is verified. [http://dx.doi.org/10.1063/1.4870243]

I. INTRODUCTION

Micro inertial fluidic switches based on electrowetting technology utilize the liquid metal mercury droplet as sensitive inertial force components to replace the traditional solid elastic electrodes. When the acceleration signal exceeds the acceleration threshold, the mercury droplet would move towards the sensitive direction and close the fixed signal electrodes.[1]

Electrowetting was first identified by Lippmann in 1857. It is a well-known phenomenon of decrease in contact angle when an external electrical potential is applied to the solid/liquid interface.[2] That is by controlling the applied voltage to change the surface tension of the droplet and to change the contact angle between the solid/liquid interface. Earlier electrowetting phenomenon is that the droplet is placed in direct contact with electrodes and it can only drive and manipulation conductive droplets. Once the applied voltage increases to some extent, the droplet would occur electrolytic reaction and generate bubble. In further research, Berge inserted a thin insulating layer between the electrolyte droplet and electrode to eliminate the problem of electrolysis, which allowed a large contact angle to be obtained by applying a higher voltage.[3] In order to distinguish with the traditional electrowetting phenomenon, this phenomenon is called electrowetting on dielectric (EWOD). In recent years, EWOD have been widely used in driving and control of droplet, display devices, optical switches and zoom optical lens and other devices.[4] The electrowetting phenomenon is also used in micro inertial fluidic switch, and the acceleration threshold of switch can be fine-tuned

[a]Author to whom correspondence should be addressed. Email: ljttlf@163.com

by controlling the contact angle between mercury droplet and dielectric layer. Through adjusting the applied voltage, we can control the contact angle.

This paper presents micro inertial fluidic switch based on electrowetting technology, the electrical wetting properties of the micro inertial fluidic switch are studied. The results show that microchannel structure parameters, applied voltage, and the mercury droplet volume have important impact on the acceleration threshold of the micro inertial fluidic switch. The worst-case analysis method is used to analyze the tolerance of the micro inertial fluidic switch and the acceleration threshold can be fine-tuned by adjusting applied voltage.

II. THE THEORETICAL BASIS OF EWOD

A considerable amount of research has been conducted on the basic principles of EWOD, device structures and its applications.Young's equation and the Lippmann-Young's equation are the basic equations in electrowetting theory. When a voltage is applied, the contact angle will decrease to a new equilibrium value, i.e., voltage can enhance wettability of the surface. Lippmann-Young's equation reveals the relationship between applied voltage and contact angle:[5]

$$\cos\theta(U) = \cos\theta_0 + \frac{\varepsilon_0\varepsilon_r}{2d\gamma_{l-g}}U^2 \tag{1}$$

Where $\theta(U)$ is the contact angle under a certain applied voltage U, θ_0 is the contact angle without applied voltage, ε_0 and ε_r are the vacuum permittivity and relative permittivity of the dielectric layer respectively, and d is the dielectric layer thickness. The right-hand side of Eq. (1) is known as the E_W number:

$$E_W = \frac{\varepsilon_0\varepsilon_r}{2d\gamma_{l-g}}U^2 \tag{2}$$

The dimensionless electrowetting number represents the ratio of the electrostatic energy to the liquid-vapor interfacial energy and reflects the ability to change the surface tension by applied an electric field.

From the Lippmann-Young's equation, the contact angle variation is related to the applied voltage and the thickness, dielectric constant of the dielectric layer. Contact angle decreases as the applied voltage increases. But in fact, when the applied voltage increases to a certain value, the further increase of voltage will not change the contact angle. This phenomenon is called contact angle saturation.[3] However, Lippmann-Young theory cannot offer rational explanation for such phenomenon. So far, there have been many interpretations for the causes of contact angle saturation. Most scholars think the charge accumulation effect of dielectric layer is the main cause of the contact angle saturation. When the applied electric field increases to a certain value, the electric charge will enter the dielectric layer and be captured by the dielectric layer. All of the increased potential is used to neutralize the charge in the dielectric layer and will not contribute to the decreases of contact angle, so that the contact angle saturation occurs. The threshold voltage increases with the increase of the thickness of dielectric layer.

Young's equation implies that the static contact angle θ_s is unique. However, this implication contradicts the experimental observations that for most material systems, the real contact angle θ can take on any value within the interval $\theta_R \leq \theta \leq \theta_A$, where θ_R and θ_A are defined as the receding and advancing angles, respectively. The difference between the two angles $\Delta\theta = \theta_A - \theta_R$ is defined as the contact angle hysteresis.[6] The smaller the contact angle hysteresis is, the faster the droplet moves on the solid surface. Many factors led to the contact line hysteresis phenomenon, for instance, the surface roughness and heterogeneity.

Under electrowetting-on-dielectric, the electrostatic forces act on the advancing contact line and the receding contact line. Wyatt C. Nelson *et al.* have studied the dynamic contact angle and hysteresis under electrowetting-on-dielectric.[7] Measurements show that if E_w or Ca (capillary number) is low, dynamic contact angle hysteresis is not affected by the EWOD voltage or the sliding speed; that is, the hysteresis increases by less than 50% with a 2 order-of-magnitude increase in sliding speed when $Ca < 10^{-3}$. If both E_w and Ca are high, the hysteresis increases with either the EWOD voltage

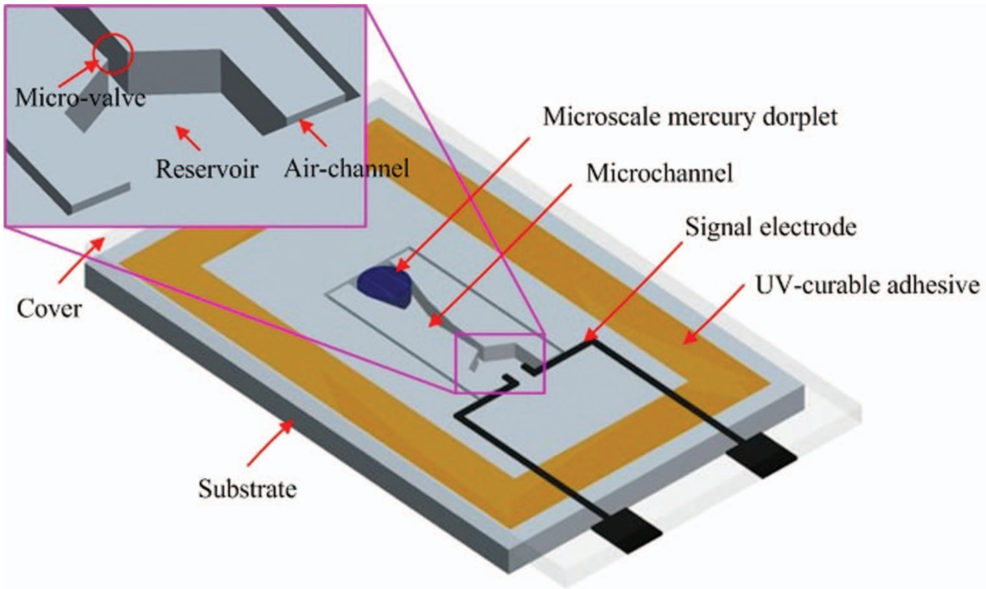

FIG. 1. Schematic of the micro inertial fluidic switch.

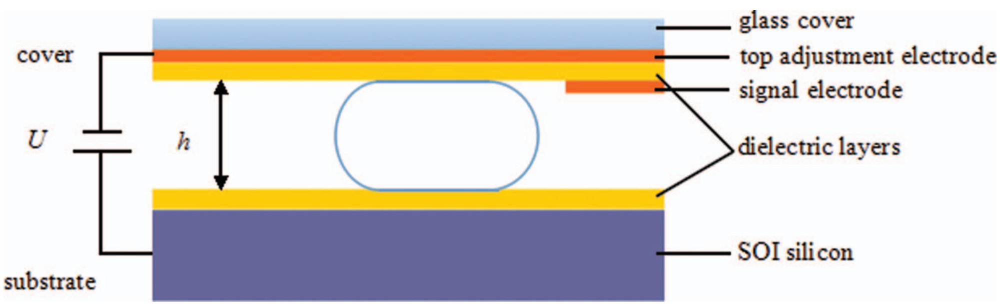

FIG. 2. The cross-sectional view of the micro inertial fluidic switch.

or the sliding speed. Ca is equal to $\mu V_{CL}/\gamma$, where μ is the viscosity, γ is the surface tension, and V_{CL} is contact line velocity.

III. THE STRUCTURE AND THEORETICAL MODEL OF MICRO-INERTIAL FLUIDIC SWITCH BASED ON ELECTROWETTING TECHNOLOGY

A. Basic structure and principle

The micro inertial fluidic switch consists of substrate, microchannel with varying rectangular cross section (microchannel with capillary valve), microscale mercury droplet, cover and air channel. The air channel is extremely useful for reducing the droplet flow resistance. Schematic and cross-sectional view of the micro inertial fluidic switch based on electrowetting technology is shown in Fig. 1 and Fig. 2, respectively. The substrate consists of SOI silicon and a dielectric layer (silicon dioxide layer) and the cover consists of the dielectric layer (silicon dioxide layer), the top adjustment electrode, signal electrode, and glass cover.

Given an applied voltage between the top adjustment electrode and SOI silicon substrate, the contact angle between the mercury droplet and the dielectric layer can be adjusted. The microscale mercury droplet is positioned in the left of micro-valve. Under the inertia force acting on the inertial switch, mercury droplet will break through the capillary micro-valve to close the signal electrodes immediately, when the acceleration is greater than the acceleration threshold. The acceleration

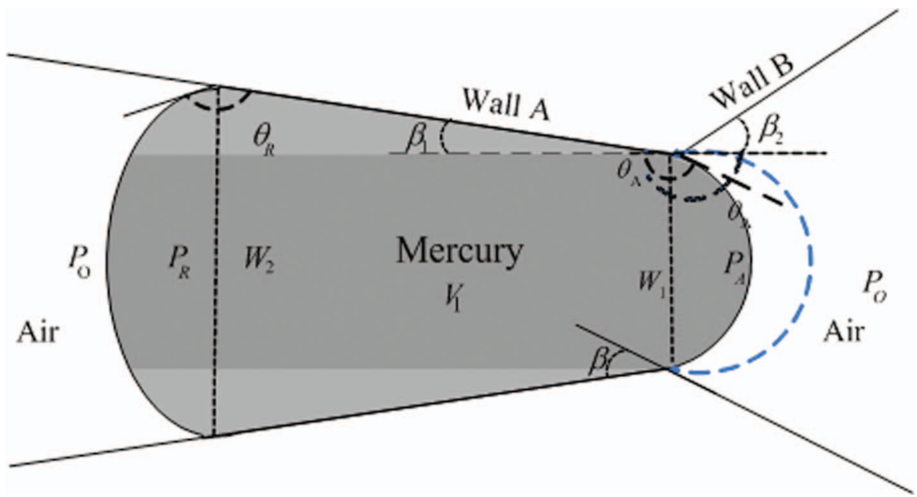

FIG. 3. The critical state of the mercury droplets through microvalve.

threshold and response time of micro inertial fluidic switch can be adjusted by changing the applied voltage, microchannel structure parameters and microscale mercury droplet volume.

B. Theoretical model of acceleration threshold

As shown in Fig. 3, under the action of lower inertia forces the mercury droplet will be stuck in the microvalve which is formed by microchannel side walls A and B. The reason is that because the contact angle β_2 between mercury advancing meniscus and the side wall B decreases and there are pressure differences between the mercury droplet and air on mercury advancing/receding meniscus. Only when the applied inertia forces overcome the resistance of additional pressure, the mercury droplet can break through the capillary microvalve (as shown in Fig. 3 with dotted lines). The above phenomenon is used in capillary passive valve to control the flow of mercury droplet, and thus the micro inertial switch has obvious threshold properties.

As liquid is free of shear force under static conditions, we assume that there is no tangential interaction between the middle mercury column (the shadow section in Fig. 3) and the neighboring liquid. The volume of shadow section can be approximated as $V_1 = 2VW_1/(W_1 + W_2)$, where V is the volume of the mercury droplet, W_1 and W_2 are the widths of micro-valve and mercury receding meniscus, respectively. Applying the Young-Laplace's equation to mercury advancing/receding meniscus, we obtain the quasi-static acceleration threshold with no voltage applied (in Ref. 8 mercury droplet contact with silicon and glass and in this paper mercury droplet contact with silicon dioxide layer, therefore the contact angles quoted from Ref. 8 are modified):[8]

$$a_{th} = \frac{2\gamma C W_1 h}{\rho V_1}\left(\frac{\cos\theta_I}{W_1} + \frac{\cos\theta_{A1}}{h} - \frac{\cos\theta_R}{W_2} - \frac{\cos\theta_{R1}}{h}\right) \tag{3}$$

$$W_2 = 2\left[\frac{\dfrac{V}{h} - S_1 + \dfrac{W_1^2}{4\tan\beta_1}}{\dfrac{\theta_R + \beta_1 - \dfrac{\pi}{2}}{\cos^2(\theta_R + \beta_1)} - |\tan(\theta_R + \beta_1)| + \dfrac{1}{\tan\beta_1}}\right]^{\frac{1}{2}} \tag{4}$$

$$S_1 = \frac{W_1^2}{4}\left[\frac{\theta_A + \beta_2 - \dfrac{\pi}{2}}{\cos^2(\theta_A + \beta_2)} - |\tan(\theta_A + \beta_2)|\right] \tag{5}$$

Where γ is the surface tension, h is the depth of microchannel, ρ is the mercury droplet density, and C is the surface roughness coefficient, which depicts contact angle hysteresis due to surface roughness. θ_I is the $\min\{\theta_A + \beta, 180^{\circ}\}$, θ_{A1} is the advancing contact angle between droplet and silicon dioxide layer in substrate, θ_R is the receding contact angle between droplet and the sidewall. θ_{R1} is the receding contact angle between droplet and silicon dioxide layer in substrate. The angles of wall A and B to the axial direction are β_1 and β_2, respectively.

IV. TOLERANCE ANALYSIS OF STRUCTURE PARAMETERS AND DROPLET VOLUME ON ACCELERATION THRESHOLD

A. The effect of applied voltage and dielectric layer thickness on acceleration threshold

The contact angle between mercury droplet and silicon dioxide layer can be adjusted by changing the applied voltage, thus making the acceleration threshold of micro inertial fluidic switch adjustable. According to the electrowetting-on-dielectric theory, the voltage applied should be kept as low as possible while obtaining the required change in contact angle, but it will increase the difficulties in design and fabrication.

According to Lippmann-Young's equation, when the change in contact angle is given, the square value of the applied voltage U is inversely proportional to the dielectric constant of the dielectric layer $\varepsilon_0\varepsilon_r$, and is proportional to the thickness of the dielectric layer d and surface tension coefficient $\gamma_{l\text{-}g}$. The equation is described as follows:

$$U^2 = \frac{2d\gamma_{l-g}\,(\cos\theta - \cos\theta_0)}{\varepsilon_0\varepsilon_r} \tag{6}$$

Therefore, to reduce the operating voltage of device, we need to use high dielectric constant material and reduce the thickness of the dielectric layer. Because the dielectric layer needs to withstand high electric field strength, the dielectric layer thickness should meet the requirements of electric insulation.

As the silicon dioxide layer is hydrophobic for the mercury droplets, it can be used as both dielectric layer and hydrophobic layer. The contact angle between mercury and silicon dioxide layer is about 135.00°. According to Ref. 9, when the voltage rises to 50.00 V, the contact angle of the mercury droplet under the 100.00-nm-thick of dioxide silicon layer is about 87.00°.[9] The contact angle almost remains unchanged as the voltage continues to increase, and the phenomenon of contact angle saturation occurs.

To avoid contact angle saturation effects, the applied voltage should be kept within 30.00 V. The electrowetting-on-dielectric effect between the mercury droplet and the dielectric layer is not only limited by the contact angle saturation effects, but also influenced by the dielectric layer breakdown. Under the same change in contact angle, the thicker the dielectric layer, the greater the applied voltage required. Thus high applied voltage and small dielectric layer thickness can increase the change in contact angle without changing the dielectric layer material and liquid material, but both of these approaches may accelerate the dielectric layer breakdown. In the case of dielectric layer breakdown, the charge will leak away through the dielectric layer, and the electrowetting phenomenon will disappear.

To obtain a large change in contact angle, the thickness of the dielectric layer should be low, but it should be greater than d_{min}. When the dielectric layer thickness is lower than d_{min}, the dielectric layer will be damaged. The breakdown field strength of the dielectric layer is approximately 2.00 MV/cm. As the maximum applied voltage is 30.00 V, to ensure that the dielectric layer breakdown phenomenon does not happen the dielectric layer thickness should be larger than 60 nm. According to Eq. (3)–(5), the dielectric layer thickness ranges from 70.00 nm to 200.00 nm and the acceleration threshold can be obtained from 13.88 g to13.10 g under the applied voltage of 20.00 V.

Assume that the average speed of mercury droplets in micro inertial fluidic switch is 0.08 m/s which is obtained from numerical simulation results, the E_{w} is 0.14 and the Ca is 2.52×10^{-4} under applied voltage the 20.00V with a 100.00 nm-thick dielectric layer. According to the Ref. 8, the influence of electrowetting on contact angle hysteresis is negligible. Thus the contact

TABLE I. The contact angle and acceleration threshold under different applied voltage.

Applied voltage	Advancing contact angle $\theta_A(U)$	Receding contact angle $\theta_R(U)$	Acceleration threshold (g)
0V	140.10°	130.40°	12.47
5V	139.33°	129.63°	12.70
10V	137.09°	127.39°	12.87
15V	133.55°	123.85°	13.16
20V	128.92°	119.22°	13.53
25V	123.37°	113.67°	13.98
30V	117.03°	107.33°	14.49

angle hysteresis under the action of electrowetting remains unchanged. Advancing contact angle θ_A is affected by the applied voltage. According to Lippmann-Young's equation, the advancing contact angle $\theta_A(U)$ under the action of electrowetting can be obtained. As the contact angle hysteresis remains unchanged with or without the applied voltage, the receding contact angle is obtained by Eq. (7).

$$\theta_R(U) = \theta_A(U) - \Delta\theta \tag{7}$$

Table I lists the contact angle and acceleration threshold under different applied voltages with a 100 nm-thick dielectric layer. When the applied voltage ranges from 0 to 30.00 V, the acceleration threshold ranges from 12.47 to 14.49 g. The results show that the acceleration threshold can be fine-tuned by adjusting the applied voltage.

Tolerance analysis is to analyze the influence of parameter variation on devices under the given parametric range of the device components. There are two ways to analyze parametric tolerance. The first is the Monte Carlo method which is a means of statistical samples, and the second is the worst-case analysis. Worst-case analysis is an analysis technique which, by accounting for component variations, determines the device performance under a worst case scenario (Under extreme environmental or operating conditions).

Acceleration threshold is one of the most important performance indexes. With no applied voltage, the structure parameters and droplet volume are important factors influencing the acceleration threshold, but the two factors are vulnerable to process errors and measuring errors. Therefore we need to consider the influence of error factors on acceleration threshold.

B. The tolerance analysis of microchannel structure parameter

According to Eq. (3)–(5), the flow characteristics of mercury droplet are not only closely related with the shape and size of microchannel as well as the droplet volume. The key structural parameters include the angles of wall A and B to the axial direction, the microchannel depth and the microvalve width.

During the fabrication process, considering the tolerance of microvalve width W_1 under worst-case conditions is 2.00 μm, the tolerance of microchannel depth h is 5.00 μm, the tolerance of the angles β_1 and β_2 of wall A and B to the axial direction are both 0.10°. That is, the nominal values of each parameter are: $W_1 = 175.00 \pm 2.00\ \mu$m, $h = 245.00 \pm 5.00\ \mu$m, $\beta_1 = 8.00 \pm 0.10°$, $\beta_2 = 70.00 \pm 0.10°$. The accuracy of micro-valve width W_1, the microchannel depth h, the angles β_1 and β_2 of wall A and B to the axial direction is 2.29%, 4.08%, 0.50% and 0.23%, respectively. Then sensitivity parameter S_i in microchannel structure parameters X_i are obtained:

$$S_1 = \left.\frac{\partial a_{th}}{\partial W_1}\right|_0 = -9.24 \times 10^4 \qquad S_2 = \left.\frac{\partial a_{th}}{\partial h}\right|_0 = 3.44 \times 10^4$$
$$S_3 = \left.\frac{\partial a_{th}}{\partial \beta_1}\right|_0 = 1.00 \qquad S_4 = \left.\frac{\partial a_{th}}{\partial \beta_2}\right|_0 = -5.00 \times 10^{-3} \tag{8}$$

Where the subscript 0 represents the nominal value of parameter. As can be seen from the Table I, when the above parameters take nominal values, the quasi-static acceleration threshold is 12.47 g with no voltage applied. The tolerance of microvalve width W_1 can be obtained as follows:

$$\frac{\Delta a_{W_1}}{a_{th}} = \frac{|S_1 \times \Delta W_1|}{a_{th}} \times 100\% = \frac{\left|-9.24 \times 10^4 \times 4 \times 10^{-6}\right|}{12.47} \times 100\% = 2.96\%$$
$$\frac{\Delta a_{h_1}}{a_{th}} = \frac{|S_2 \times \Delta h|}{a_{th}} \times 100\% = \frac{\left|3.44 \times 10^4 \times 10 \times 10^{-6}\right|}{12.47} \times 100\% = 2.76\%$$
$$\frac{\Delta a_{\beta_1}}{a_{th}} = \frac{|S_3 \times \Delta \beta_1|}{a_{th}} \times 100\% = \frac{|1.00 \times 0.2|}{12.47} \times 100\% = 1.60\%$$
$$\frac{\Delta a_{\beta_2}}{a_{th}} = \frac{|S_4 \times \Delta \beta_2|}{a_{th}} \times 100\% = \frac{\left|-5.00 \times 10^{-3} \times 0.2\right|}{12.47} \times 100\% = 0.01\% \tag{9}$$

The above equations indicate that the acceleration threshold tolerance are 2.96%, 2.76%, 1.6% and 0.01% under the accuracy of micro-valve width W_1, the microchannel depth h, the angles β_1 and β_2 of wall A and B to the axial direction is 2.29%, 4.08%, 0.50% and 0.23%, respectively.

C. The tolerance analysis of the mercury droplet volume

When the mercury droplet is placed on the solid surface, Eq. (10) is used to estimate the mercury droplet volume.

$$V = \frac{\pi R^3}{3}\left(2 - 3\cos\theta + \cos^3\theta\right) \tag{10}$$

Where, R represents the radius of the contact area and θ represents the contact angle between droplet and solid surface.

In practice, it is difficult to accurately control the droplet volume. First, the volume of droplet must be estimated. Then the mercury droplet is put into the micro inertial fluidic switch to test and the measuring error is introduced.

Assuming that the tolerance of the mercury droplet contact diameter R under worst-case conditions is 2.00 μm, according to Eq. (10), the rate of change in volume caused by measurement error of contact radius R is 3.20% and the acceleration threshold tolerance is 2.62%.

D. The total tolerance analysis on acceleration threshold

Therefore, under worst-case condition the total acceleration threshold tolerance caused by various errors can be calculated by the following formula:

$$\left.\frac{\Delta a_{th}}{a_{th}}\right|_0 = 2.96\% + 2.76\% + 1.60\% + 0.01\% + 2.62\% = 9.95\% \tag{11}$$

Therefore, the acceleration threshold ranges from 11.23 to 13.71. In the presence of process errors and measuring errors, there is a deviation between test acceleration threshold and target acceleration threshold. The target acceleration threshold can be achieved by fine-tuning the applied voltage.

Assuming that the target threshold of the micro inertial fluidic switch is 13.50 g and the acceleration threshold tolerance is controlled within 3%, the acceleration threshold can be fine-tuned in the range of 13.10 g to 13.91 g. According to Eq. (3)–(5), the applied voltage can be adjusted in the range of 14.00 to 24.2 V to achieve the target acceleration threshold of 13.50 g.

V. CONCLUSIONS

Micro inertial fluidic switches based on electrowetting technology utilize the liquid metal mercury droplet as sensitive inertial force components to replace the traditional solid elastic electrodes.

The advantages are no moving parts, low contact resistance, the adjustable acceleration threshold and so on. In this paper, the electricalwetting properties of micro inertial fluidic switch are studied and the results show that the factors, such as microchannel structure parameters, applied voltage, mercury droplet volume, have significant effect on switch acceleration threshold. As the uncertainty in process and the existence of measuring errors, worst-case analysis is used to analyze the tolerance of the micro inertial fluidic switch. The acceleration threshold tolerance are 2.96%, 2.76%, 1.60% and 0.01% under the accuracy of micro-valve width W_1, the microchannel depth h, the angles β_1 and β_2 of wall A and B to the axial direction is 2.29%, 4.08%, 0.50% and 0.23%, respectively. The rate of change in volume caused by measurement error of contact radius R is 3.20% and the acceleration threshold tolerance is 2.62%. To achieve the target acceleration threshold, we could fine-tune the applied voltage while keeping the microchannel structural parameters, the droplet volume and the dielectric layer thickness constant. The trimming method of acceleration threshold is verified in this paper. The results of the study can provide a reference for the area of new micro inertial switch.

ACKNOWLEDGMENTS

This work is supported by NSAF under Grant No.11076024 and Major Project of Education Department in Sichuan under Grant No.11ZA216.

[1] K. Yoo, U. Park, and J. Kim, "Development and characterization of a novel configurable MEMS inertial switch using a microscale liquid-metal droplet in a microstructured channel," Sensors and Actuators A : Physical **166**(2), 234–240 (2011).
[2] Rui Zhao, Zhong-cheng Liang, Bo Jiang, Rong-qing Xu *et al.*, "Studies on electrowetting of room temperature ionic liquids," Optik-International Journal for Light and Electron Optics **214**(20), 4089–4091 (2013).
[3] Frieder Mugele, "Jean-Christophe Baret. Electrowetting: from basics to applications," Journal of physics: condensed matter **17**(28), 705–774 (2005).
[4] Ya-Pu Zhao and Ying Wang, "Fundamentals and applications of electrowetting: a critical review," Reviews of Adhesion and Adhesives **1**(1), 114–174 (2013).
[5] Nah-Young Kim, Sung-Min Hong, and Soon-Sup Park, "The movement of micro droplet with the effects of dielectric layer and hydrophobic surface treatment with R.F. atmospheric plasma in EWOD structure," Journal of Physics: Conference Series **34**, 650–655 (2006).
[6] Chen Fang, Carlos Hidrovo, Fu-min Wang, John Eaton *et al.*, "3-D numerical simulation of contact angle hysteresis for microscale two phase flow," International Journal of Multiphase Flow **34**, 690–705 (2008).
[7] Wyatt C. Nelson, Prosenjit Sen, and Chang-Jin Kim, "Dynamic contact angles and hysteresis under electrowetting-on-dielectric," Langmuir **27**(16), 10319–10326 (2011).
[8] Yi Lin, Tao Yang, Ting Ting Liu, Guang Yan Chen *et al.*, "Analysis and simulation of micro-fluidic inertial switch," Key Engineering Materials **503**, 348–353 (2012).
[9] Liu Ke, "Preparation and wetting of porous silicon," Shenyang institute of aeronautical engineering, 2012.